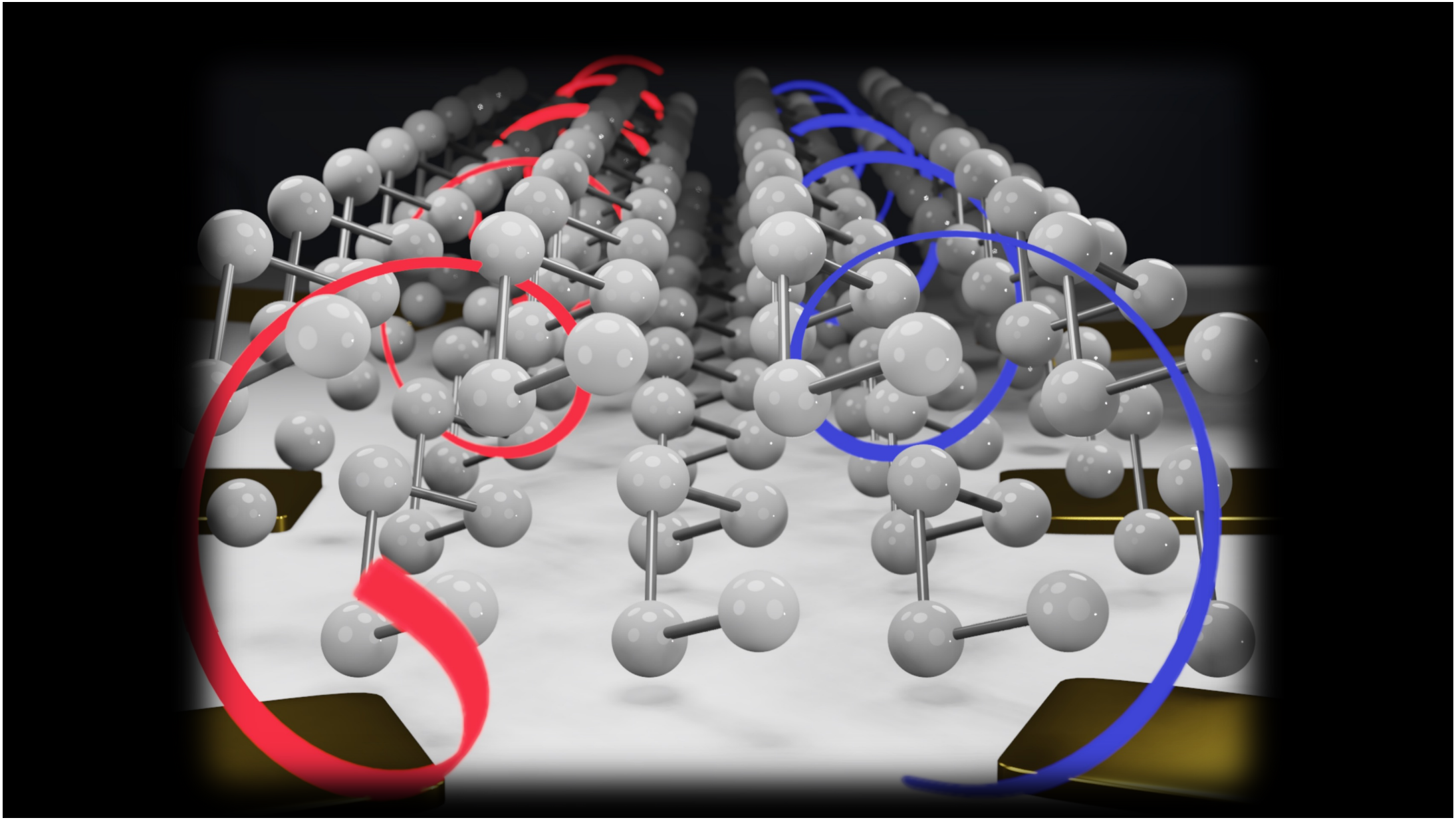

CIC
nanoGUNE
MEMBER OF BASQUE RESEARCH & TECHNOLOGY ALLIANCE
Non-linear electronic transport in chiral Te
Luis E. Hueso
GOBIERNO DE ESPAÑA
MINISTERIO DE CIENCIA E INNOVACIÓN
EXCELENCIA MARÍA DE MAEZTU
ikerbasque
Basque Foundation for Science
HORIZON 2020
HORIZON EUROPE
"la Caixa" Foundation
intel





AGH University Krakow
Witold Skowronski
Kamil Staszek

CFM San Sebastian
Ivo Souza
Stepan S. Tsirkin

DIPC San Sebastian
Fernando de Juan

Halle University
Annika Johansson
Ingrid Mertig

Laboratory Albert Fert
Albert Fert

GOBIERNO DE ESPAÑA MINISTERIO DE CIENCIA E INNOVACIÓN
AGENCIA ESTATAL DE INVESTIGACIÓN
EXCELENCIA MARÍA DE MAEZTU
ikerbasque Basque Foundation for Science
THE FRAMEWORK PROGRAMME FOR RESEARCH AND INNOVATION HORIZON 2020
HORIZON EUROPE
Marie Skłodowska-Curie Actions
"la Caixa" Foundation
intel

Outline

- Electronic transport
- The case study: Chiral Te
- Non-linear conductivity in Te
- Non-linear magnetoconductivity in Te
- Conclusions

Electronic transport

$$V = R^{(1,0)}I + R^{(1,2)}IB^2 + R^{(1,1)}IB + R^{(2,1)}I^2B + R^{(2,0)}I^2$$

- $R^{(1,0)}I$: Ohmic resistance
- $R^{(1,2)}IB^2$: Ordinary magnetoresistance
- $R^{(1,1)}IB$: Hall resistance
- $R^{(2,1)}I^2B$: Non-linear magnetoconductivity
- $R^{(2,0)}I^2$: Non-linear conductivity

✓ $\mathcal{P}$-symmetry

× $\mathcal{P}$-symmetry

M. Suarez-Rodriguez, LEH *et al.*, *Nat. Mater.* **24**, 1005 (2025)

Electronic transport

Centrosymmetric conductor

$$V = R^{(1,0)}I + R^{(1,2)}IB^2 + R^{(1,1)}IB$$

Linear transport

$R(I) = R(-I)$

Non-centrosymmetric conductor

$$V = R^{(1,0)}I + R^{(1,2)}IB^2 + R^{(1,1)}IB + R^{(2,1)}I^2B + R^{(2,0)}I^2$$

Non-linear magnetoconductivity (NLMC)

$R(I,B) \neq R(-I,B)$ and $R(I,B) \neq R(I,-B)$

Non-linear conductivity (NLC)

$R(I) \neq R(-I)$

AC current $(I^\omega) \longrightarrow$

$$V^\omega = R^{(1,0)}I^\omega + R^{(1,2)}I^\omega B^2 + R^{(1,1)}I^\omega B$$

$$V^{2\omega} = R^{(2,1)}(I^\omega)^2 B + R^{(2,0)}(I^\omega)^2$$

M. Suarez-Rodriguez, LEH *et al.*, *Nat. Mater.* **24**, 1005 (2025)

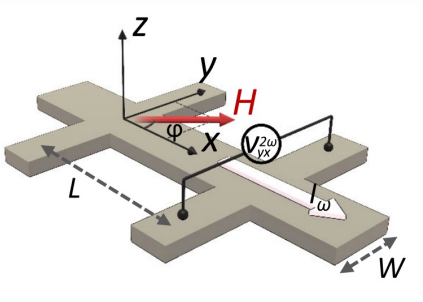
Electronic transport Non-linear magnetoconductivity (NLMC)

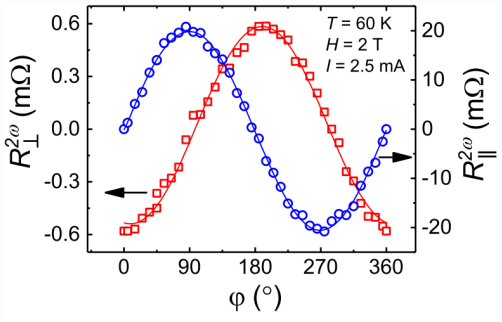
$$V^{2\omega} = R^{(2,1)}(I^{\omega})^2 B \longrightarrow R^{2\omega} = \frac{V^{2\omega}}{I^{\omega}} = R^{(2,1)} I^{\omega} B$$

Longitudinal NLMC Bilinear magnetoresistance and Unidirectional magnetoresistance

Transverse NLMC Non-linear planar Hall effect

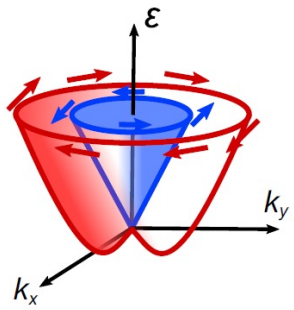
Topological insulators (TIs)

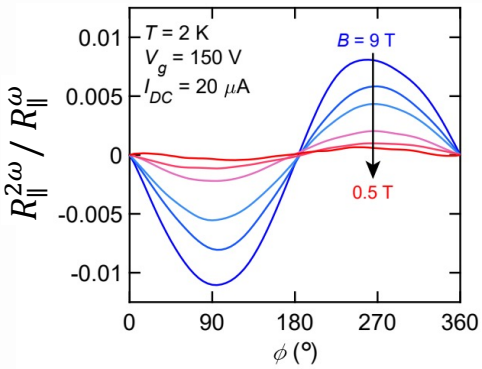




He *et al.*, *Phys. Rev. Lett.* **123**, 016801 (2019)

2D electron gases (2DGs)





Vaz et al., *Phys. Rev. Mater.* **4**, 071001 (2020)

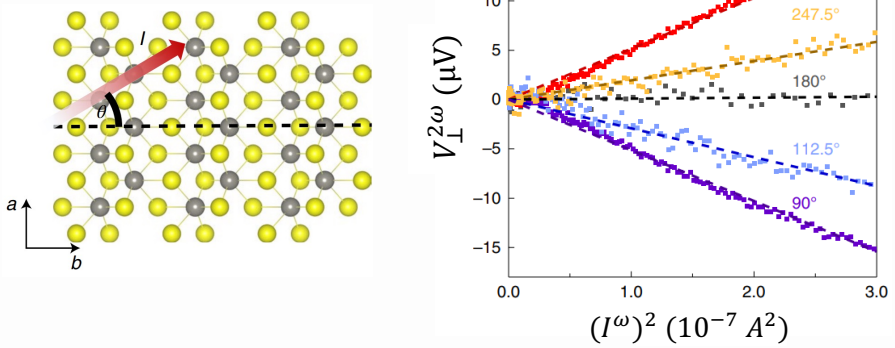
Electronic transport Non-linear conductivity (NLC)

$$V^{2\omega} = R^{(2,0)}(I^{\omega})^2$$

Transverse NLC Non-linear Hall effect (NLHE)

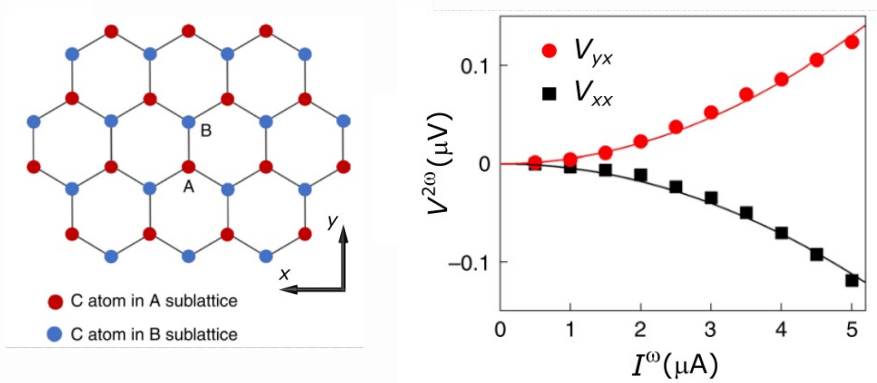
Longitudinal NLC

WTe_2



Kang *et al., Nat. Mater.* **18**, 324 (2019)

hBN/Graphene/hBN heterostructure



He *et al., Nat. Nanotechnol.* **17**, 378 (2022)

Electronic transport

		Material	Conf.	$V^{2\omega}$ (μV)	I^{ω} (μA)		Trange (K)	$\rho^{(1,0)}$($\mu\Omega m$)	$\sigma^{(2,0)}$ ($A\,V^{-2}$)	$\rho^{(2,0)}$ ($VA^{-2}m^{-3}$)
Polar	NLC	WTe_2	Trans	60	1		10-100 (10)	1	1.57E+00	1.57E+00
		WTe_2	Trans	30	740		2-100 (1.8)	1.7	5.69E-06	2.80E-05
		WTe_2	Trans	9	8		80	-	-	-
		$MoTe_2$	Trans	125	97		10-100 (10)	2.5	1.87E-03	2.93E-02
		$MoTe_2$	Trans	0.4	10000		2-40 (2)	0.01	7.95E+00	7.95E-06
		$NbIrTe_4$	Trans	20	280		2-300 (2)	0.03	3.54E+02	9.57E-03
		BiTeBr	Trans	2000	2		20-350 (50)	32	3.05E-02	1.00E+03
		$BaMnSb_2$	Trans	400	200		100-400 (240)	100	2.86E-06	2.86E+00
		Material	**Conf.**	$V^{2\omega}$ (μV)	I^{ω} (μA)	B (T)	Trange (K)	$\rho^{(1,0)}$($\mu\Omega m$)	$\sigma^{(2,1)}$($AV^{-2}T^{-1}$)	$\rho^{(2,1)}$($VA^{-2}m^{-3}T^{-1}$)
	NLMC	WTe_2	Long	36	1200	14	2-300 (300)	6	1.19E-06	2.58E-04
		WTe_2	Long	0.7	40	7	10-200 (10)	30	1.13E-07	3.04E-03
		WTe_2	Long	0.81	9000	1	2-100 (5)	0.05	1.26E+08	1.57E+04
		WTe_2	Trans	0.23	9000	1	2-100 (5)	0.1	6.18E+06	6.18E+03
		WTe_2	Trans	8	400	9	100	0.43	3.76E-02	2.99E-03
		BiTeBr	Long	1	80	9	2-200 (2)	20	2.17E-05	1.74E-01
Chiral		**Material**	**Conf.**	$V^{2\omega}$ (μV)	I^{ω} (μA)		Trange (K)	$\rho^{(1,0)}$($\mu\Omega m$)	$\sigma^{(2,0)}$ ($A\,V^{-2}$)	$\rho^{(2,0)}$ ($VA^{-2}m^{-3}$)
	NLC	Te	Long	1200	1		10-100 (10)	700	7.13E-04	2.45E+05
		Material	**Conf.**	$V^{2\omega}$ (μV)	I^{ω} (μA)	B (T)	Trange (K)	$\rho^{(1,0)}$($\mu\Omega m$)	$\sigma^{(2,1)}$($AV^{-2}T^{-1}$)	$\rho^{(2,1)}$($VA^{-2}m^{-3}T^{-1}$)
	NLMC	Te	Long	650	1	9	2-100 (10)	810	5.50E-04	2.93E+05
		Te	Trans	25	1	9	50-150 (50)	1810	8.28E-07	4.91E+03
		Te	Long	33.6	5	3	0.1 (0.1-15)	1.92	5.06E+00	3.58E+01
		Te	Trans	20	12	18	1.5	1.92	6.98E-02	4.94E-01
Surfaces and interfaces		**Material**	**Conf.**	$V^{2\omega}$ (μV)	I^{ω} (μA)		Trange (K)	$\rho^{(1,0)}$($\mu\Omega m$)	$\sigma^{(2,0)}$ ($A\,V^{-2}$)	$\rho^{(2,0)}$ ($VA^{-2}m^{-3}$)
	NLC	Te	Trans	148000	10		200-300 (100)	300	1.07E-03	2.89E+04
		Bi_2Se_3	Trans	15	1500		20-200 (20)	0.38	4.48E-04	2.46E-05
		$TaIrTe_4$	Trans	120	650		2-300 (300)	3	1.40E-03	3.79E-02
		$Pb_{1-x}Sn_xTe$	Trans	1000	30		5-300 (5)	420	-	-
		Bi(111)	Trans	0.6	60		283-333 (300)	7.5	4.17E-05	4.17E-02
		Material	**Conf.**	$V^{2\omega}$ (μV)	I^{ω} (μA)	B (T)	Trange (K)	$\rho^{(1,0)}$($\mu\Omega m$)	$\sigma^{(2,1)}$($AV^{-2}T^{-1}$)	$\rho^{(2,1)}$($VA^{-2}m^{-3}T^{-1}$)
	NLMC	Ge (111)	Long	3000	10	1	2-300 (15)	10000	9.00E-04	9.00E+08
		Bi_2Se_3	Long	5	100	9	2-300 (60)	6.5	2.98E-04	8.19E-02
		Bi_2Se_3	Trans	5.2	4000	3	2-70 (60)	5	6.93E-06	8.67E-04
		$LaAlO_3/SrTiO_3$	Long	20	20	9	2	0.07	5.40E+00	1.85E-03
		$SrTiO_3$ (001)	Long	40	1000	1	2-70 (2)	1	1.17E-01	1.17E-01
		$SrTiO_3$ (001)	Trans	10	1250	1.5	2-70 (2)	1	7.18E-02	7.18E-02
		$SrTiO_3$ (111)	Long	48	300	0.12	2-80 (7)	0.42	8.35E+01	6.18E+00
		$(Bi_{1-x}Sb_x)Te_3$	Long	6	0.3	0.16	0.03-7 (0.08)	34	3.62E-02	1.42E+03
Engineered structures		**Material**	**Conf.**	$V^{2\omega}$ (μV)	I^{ω} (μA)		Trange (K)	$\rho^{(1,0)}$($\mu\Omega m$)	$\sigma^{(2,0)}$ ($A\,V^{-2}$)	$\rho^{(2,0)}$ ($VA^{-2}m^{-3}$)
	NLC	hBN-MLG-hBN	Long	800	4.5		1.7-120 (1.7)	0.023	1.88E+05	2.28E+00
		hBN-MLG-hBN	Trans	600	4.5		1.7-120 (1.7)	0.023	1.41E+05	1.71E+00
		t-BLG	Trans	13	0.15		1.5-70(1.5)	0.043	1.40E+08	1.11E+01
		t-BLG	Trans	1000	1		1.7-80 (1.7)	0.54	7.34E+02	1.16E+02
		t-dBLG	Trans	100	1		1.7-20 (1.7)	0.07	3.70E+05	1.27E+02
		t-TLG	Long	5	0.1		0.02	0.042	5.62E+05	4.17E+01
		t-TLG	Trans	3	0.1		0.02	0.042	3.37E+05	2.50E+01
		Strained-BLG	Trans	1.2	0.1		1.5-15(5)	4.12	3.36E-01	2.35E+01
		Strained-WSe_2	Trans	10	4.5		5-140(140)	0.43	7.95E-01	6.32E-02
		t-WSe_2	Trans	25000	0.000006		1.5-30 (1.5)	4.8	4.19E+12	4.63E+14
		WSe_2-WTe_2	Trans	1500	1		25-100 (25)	22.5	2.96E-01	3.38E+03
Magnetic		**Material**	**Conf.**	$V^{2\omega}$ (μV)	I^{ω} (μA)		Trange (K)	$\rho^{(1,0)}$($\mu\Omega m$)	$\sigma^{(2,0)}$ ($A\,V^{-2}$)	$\rho^{(2,0)}$ ($VA^{-2}m^{-3}$)
	Anomalous NLMC	5L-$MnBi_2Te_4$	Trans	250	5		11	22	5.29E-02	5.63E+02
		6L-$MnBi_2Te_4$	Trans	300	10		1.8-22 (1.8)	55	2.54E-04	4.23E+01
		4L-$MnBi_2Te_4$	Long	300	10		1.8-200 (1.8)	35	7.57E-04	3.24E+01
		4L-$MnBi_2Te_4$	Trans	400	10		1.8-200 (1.8)	35	1.26E-03	5.41E+01
		CuMnAs	Trans	330	2000		-	1	4.95E-03	4.95E-03
		Mn_3Sn/Pt	Trans	35	4500		100-320 (300)	3.5	1.81E-05	7.78E-04
		CrSBr (FM)	Long	2000	1		2-140 (2)	3.52	2.84E+02	1.24E+04
		CrSBr (AFM)	Long	1000	1		2-140 (2)	1.76	1.14E+03	6.20E+03

Electronic transport Symmetry origin

Point Group	NLC									NLMC								
	Longitudinal			Transverse						Longitudinal			Transverse					
	xx	*yy*	*zz*	*xy*	*xz*	*yx*	*yz*	*zx*	*zy*	*xx*	*yy*	*zz*	*xy*	*xz*	*yx*	*yz*	*zx*	*zy*
1	✓	✓	✓	✓	✓	✓	✓	✓	✓	*x,y,z*	*x,y,z*	*x,y,z*	*x,y,z*	*x,y,z*	*x,y,z*	*x,y,z*	*x,y,z*	*x,y,z*
$\bar{1}$	×	×	×	×	×	×	×	×	×	×	×	×	×	×	×	×	×	×
2	×	✓	×	×	×	✓	✓	×	×	*x,z*	*y*	*x,z*	*x,z*	*x,z*	*y*	*y*	*x,z*	*x,z*
m	✓	×	✓	✓	✓	×	×	✓	✓	*y*	*x,z*	*y*	*y*	*y*	*x,z*	*x,z*	*y*	*y*
2/m	×	×	×	×	×	×	×	×	×	×	×	×	×	×	×	×	×	×
222	×	×	×	×	×	×	×	×	×	*x*	*y*	*z*	*x*	*x*	*y*	*y*	*z*	*z*
mm2	×	×	✓	×	×	×	×	✓	✓	*y*	*x*	×	*y*	*y*	*x*	*x*	×	×
mmm	×	×	×	×	×	×	×	×	×	×	×	×	×	×	×	×	×	×
4	×	×	✓	×	×	×	×	✓	✓	*x,y*	*x,y*	*z*	*x,y*	*x,y*	*x,y*	*x,y*	*z*	*z*
$\bar{4}$	×	×	×	×	×	×	×	✓	✓	*x,y*	*x,y*	×	*x,y*	*x,y*	*x,y*	*x,y*	*z*	*z*
4/m	×	×	×	×	×	×	×	×	×	×	×	×	×	×	×	×	×	×
422	×	×	×	×	×	×	×	×	×	*x*	*y*	*z*	*x*	*x*	*y*	*y*	*z*	*z*
4mm	×	×	✓	×	×	×	×	✓	✓	*y*	*x*	×	*y*	*y*	*x*	*x*	×	×
$\bar{4}2m$	×	×	×	×	×	×	×	×	×	*x*	*y*	×	*x*	*x*	*y*	*y*	*z*	*z*
4/mmm	×	×	×	×	×	×	×	×	×	×	×	×	×	×	×	×	×	×
3	✓	✓	✓	✓	×	✓	×	✓	✓	*x,y,z*	*x,y,z*	*z*	*x,y,z*	*x,y*	*x,y,z*	*x,y*	*x,y,z*	*x,y,z*
$\bar{3}$	×	×	×	×	×	×	×	×	×	×	×	×	×	×	×	×	×	×
32	✓	×	×	✓	×	×	×	×	×	*x*	*y,z*	*z*	*x*	*x*	*y,z*	*y*	*y,z*	*y,z*
3m	×	✓	✓	×	×	✓	×	✓	✓	*y,z*	*x,z*	×	*y,z*	*y*	*x*	*x*	*x*	*x*
$\bar{3}m$	×	×	×	×	×	×	×	×	×	×	×	×	×	×	×	×	×	×
6	×	×	✓	×	×	×	×	✓	✓	*x,y*	*x,y*	*z*	*x,y*	*x,y*	*x,y*	*x,y*	*z*	*z*
$\bar{6}$	✓	✓	×	✓	×	✓	×	×	×	*z*	*z*	×	*z*	×	*z*	×	*x,y*	*x,y*
6/m	×	×	×	×	×	×	×	×	×	×	×	×	×	×	×	×	×	×
622	×	×	×	×	×	×	×	×	×	*x*	*y*	*z*	*x*	*x*	*y*	*y*	*z*	*z*
6mm	×	×	✓	×	×	×	×	✓	✓	*y*	*x*	×	*y*	*y*	*x*	*x*	×	×
$\bar{6}m2$	×	✓	×	×	×	✓	×	×	×	*z*	×	×	*z*	×	×	×	*x*	*x*
6/mmm	×	×	×	×	×	×	×	×	×	×	×	×	×	×	×	×	×	×
23	×	×	×	×	×	×	×	×	×	*x*	*y*	*z*	*x*	*x*	*y*	*y*	*z*	*z*
$m\bar{3}$	×	×	×	×	×	×	×	×	×	×	×	×	×	×	×	×	×	×
432	×	×	×	×	×	×	×	×	×	*x*	*y*	*z*	*x*	*x*	*y*	*y*	*z*	*z*
$\bar{4}3m$	×	×	×	×	×	×	×	×	×	×	×	×	*x*	*x*	*y*	*y*	*z*	*z*
$m\bar{3}m$	×	×	×	×	×	×	×	×	×	×	×	×	×	×	×	×	×	×

Detection direction

Stimulus direction

M. Suarez-Rodriguez, LEH *et al.*, *Nat. Mater.* **24**, 1005 (2025)

Outline

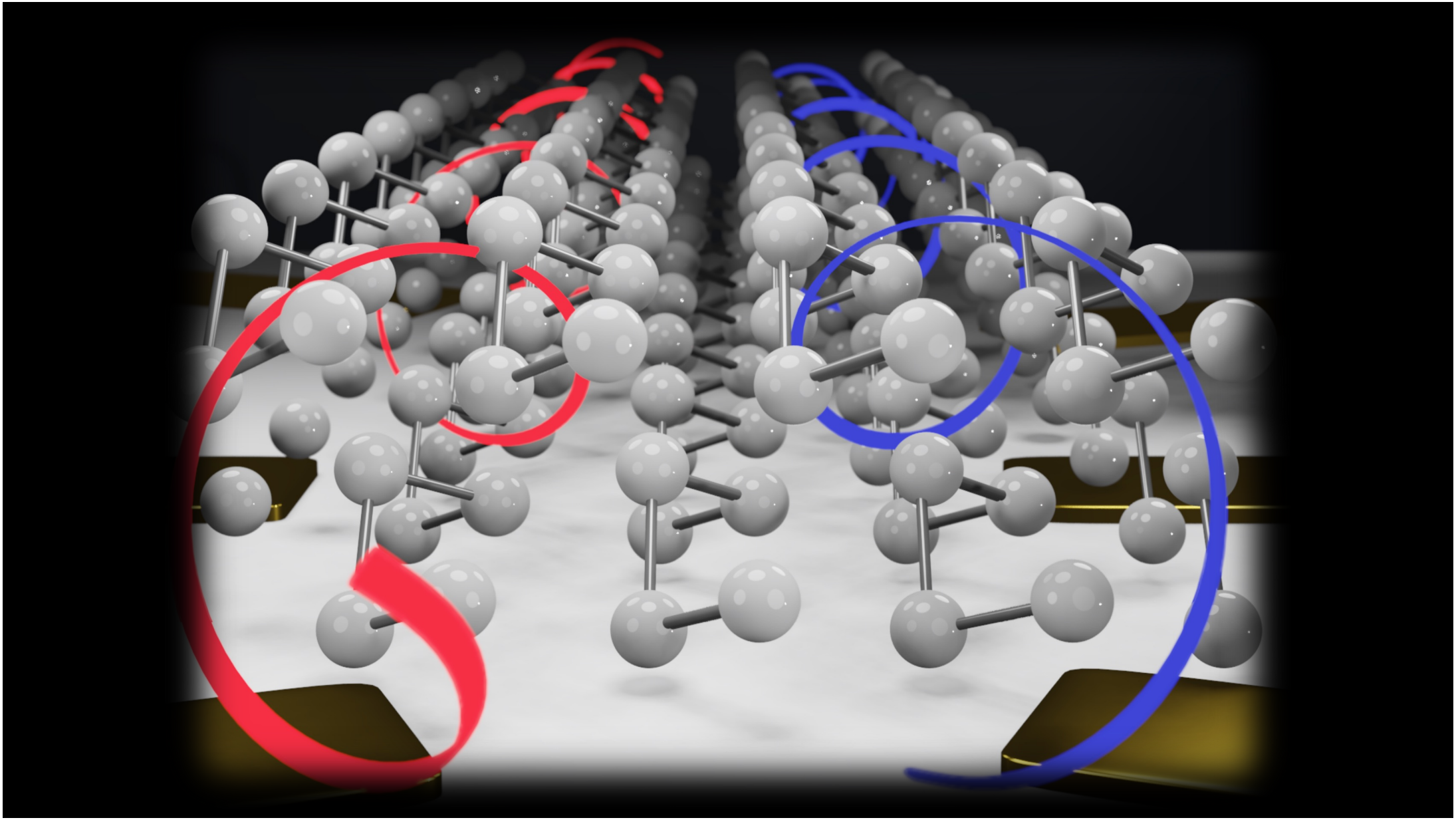
Electronic transport

The case study: Chiral Te

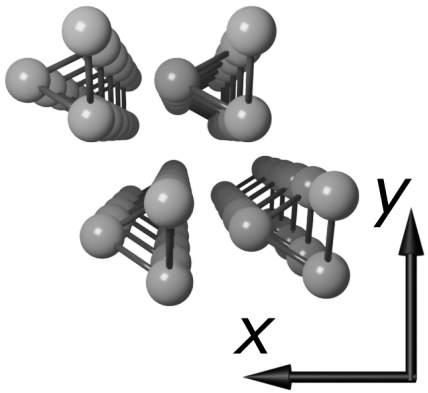
Non-linear conductivity in Te

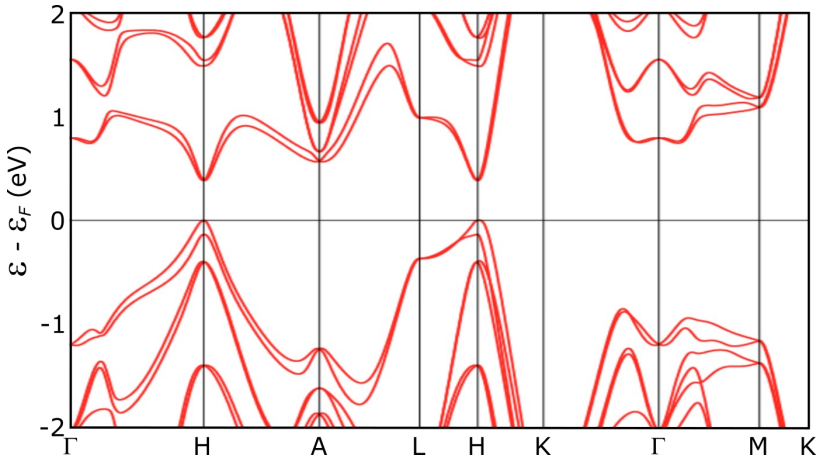
Non-linear magnetoconductivity in Te

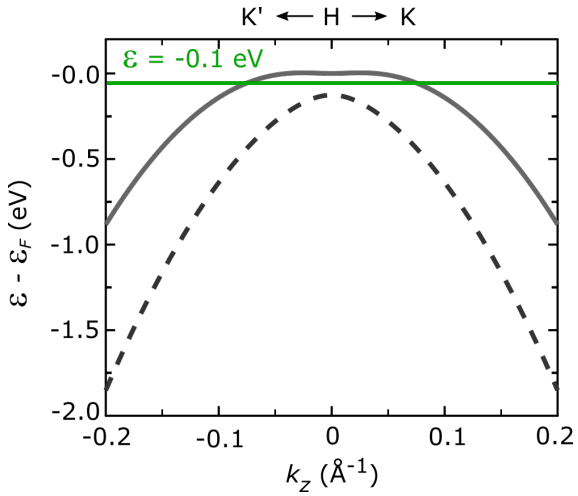
Conclusions



Chiral Te Crystal & band structure





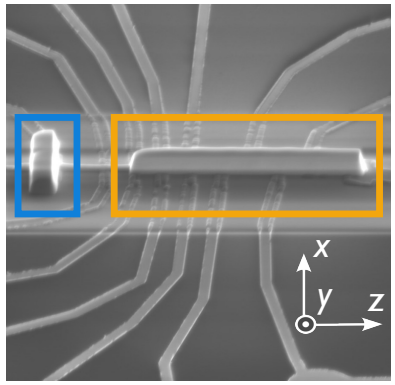


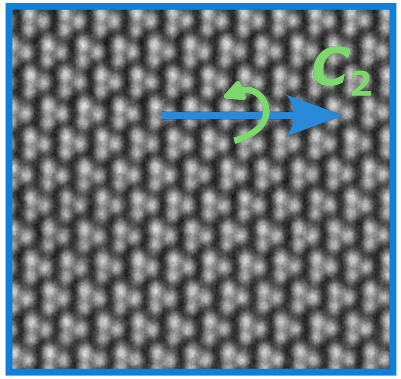
Strong crystal anisotropy

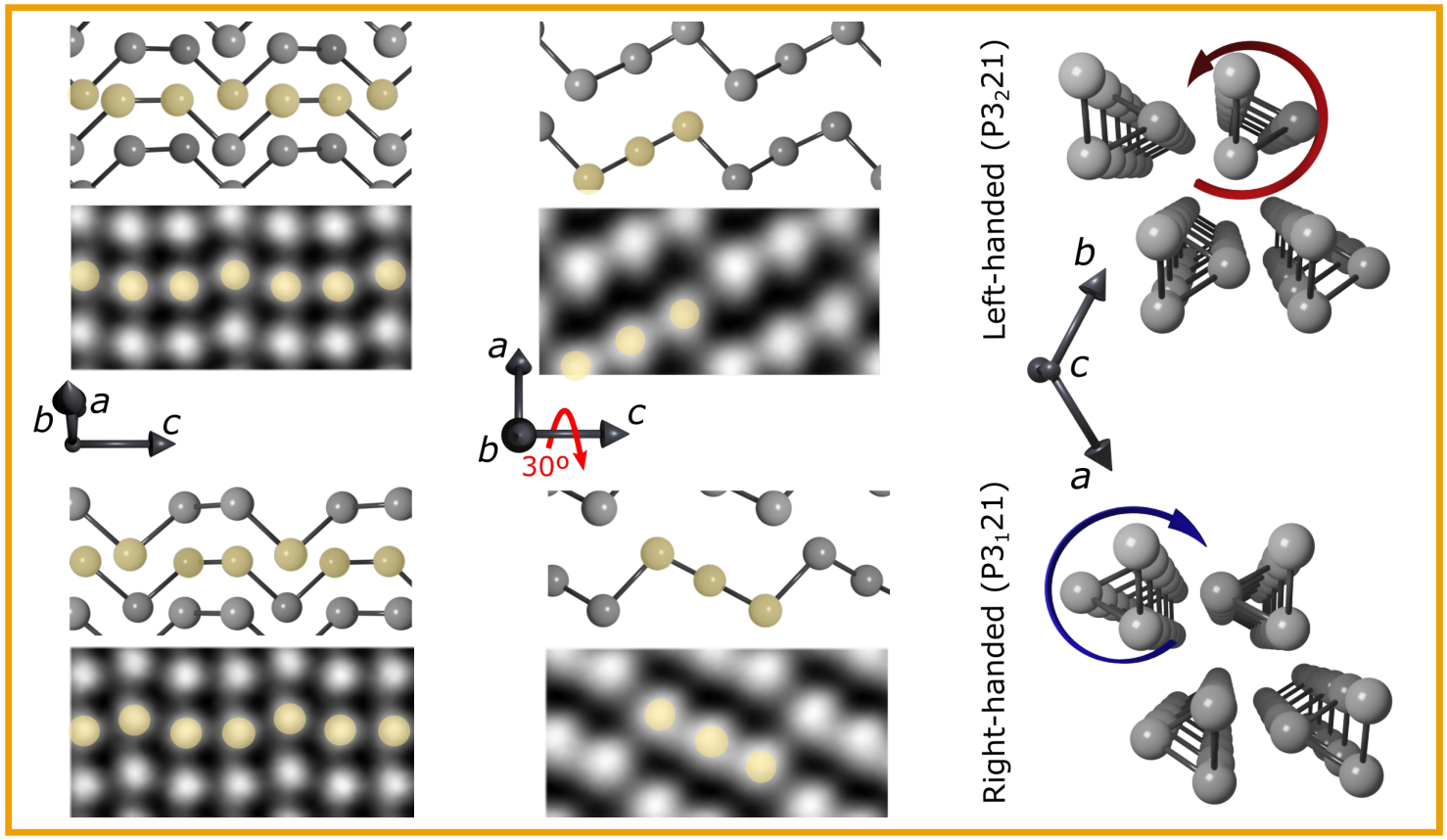
- × $\mathcal{P}$-symmetry
- × Mirror symmetry

Degenerate semiconductor

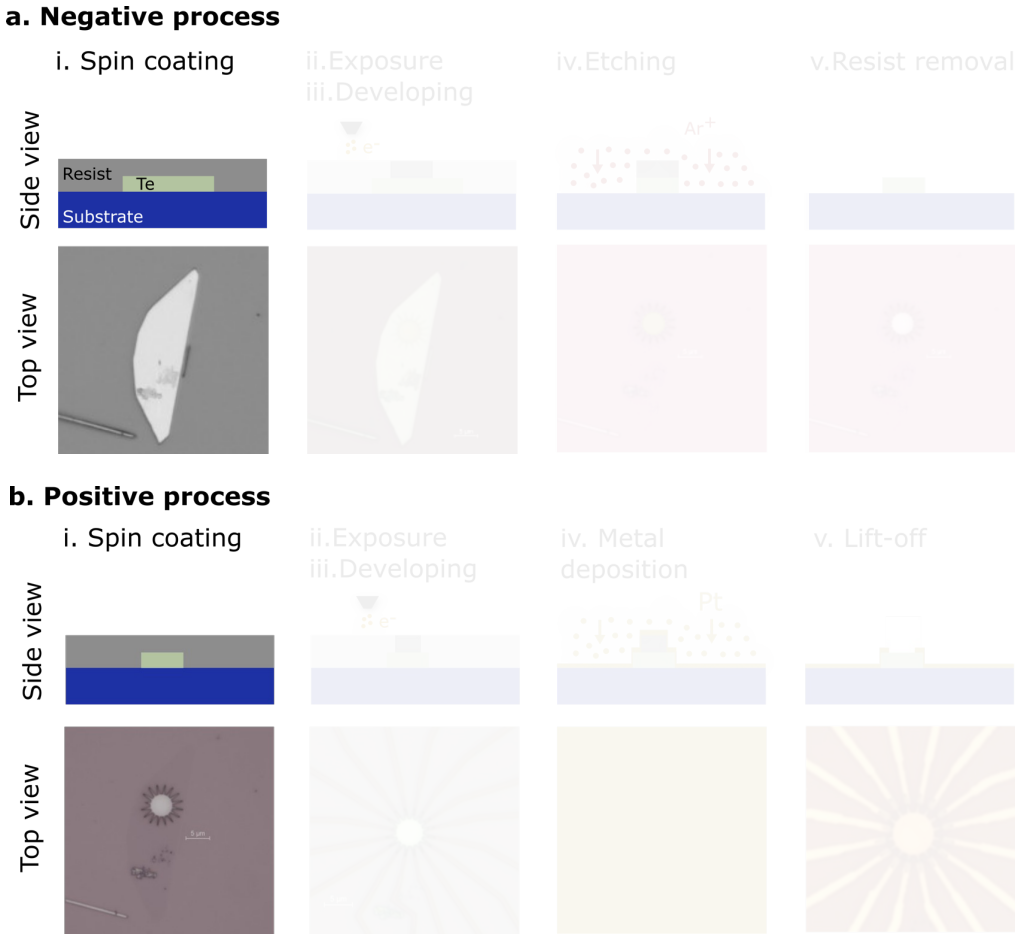
Chiral Te Crystal orientations & handedness determination

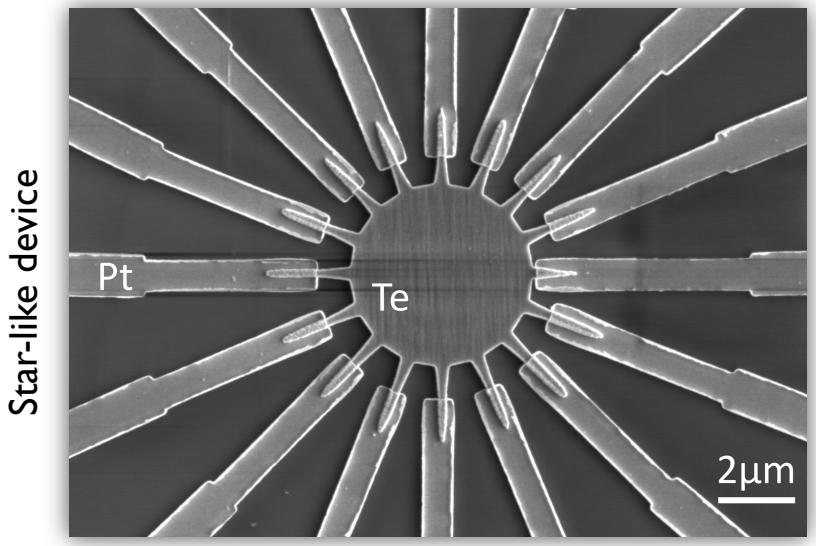






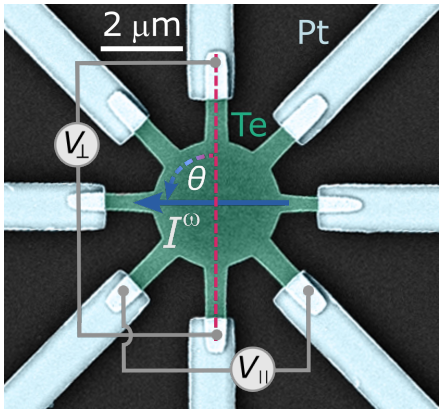
Chiral Te Device fabrication

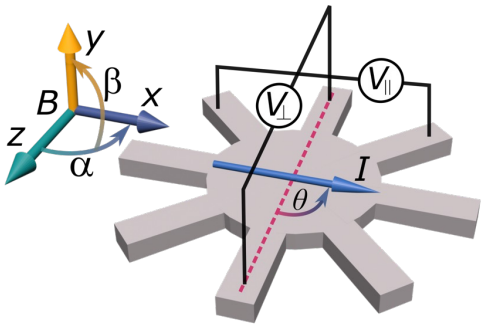


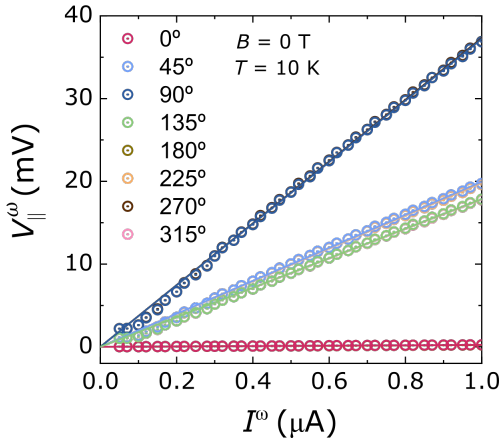


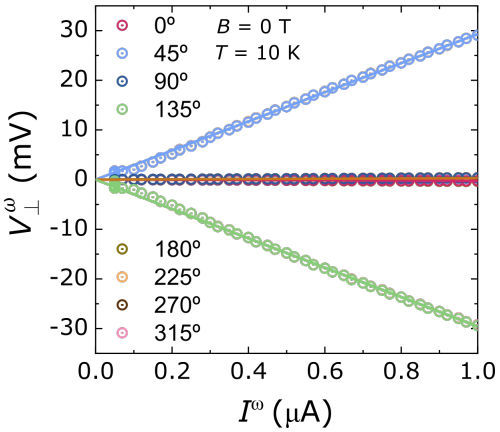
Chiral Te Linear transport

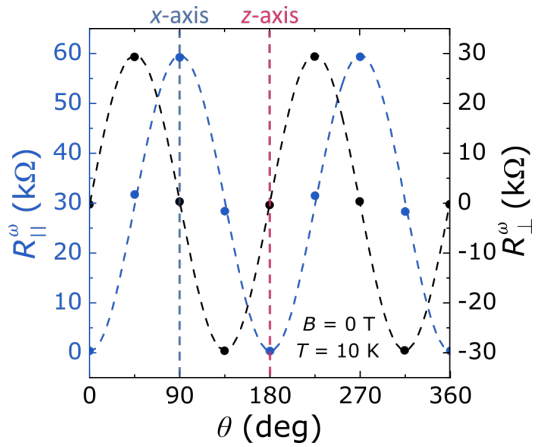
$$V^{\omega} = R^{(1,0)} I^{\omega} \longrightarrow \begin{cases} R_{\parallel}^{\omega} = V_{\parallel}^{\omega}/I^{\omega} = R_{xx}^{(1,0)} cos^2(\theta) + R_{zz}^{(1,0)} sin^2(\theta) \\ R_{\perp}^{\omega} = V_{\perp}^{\omega}/I^{\omega} = \left(R_{xx}^{(1,0)} - R_{zz}^{(1,0)}\right) sin(\theta)\cos(\theta) \end{cases}$$











Outline

Electronic transport

The case study: Chiral Te

Non-linear conductivity in Te

Non-linear magnetoconductivity in Te

Conclusions

NLC in Te Symmetry origin

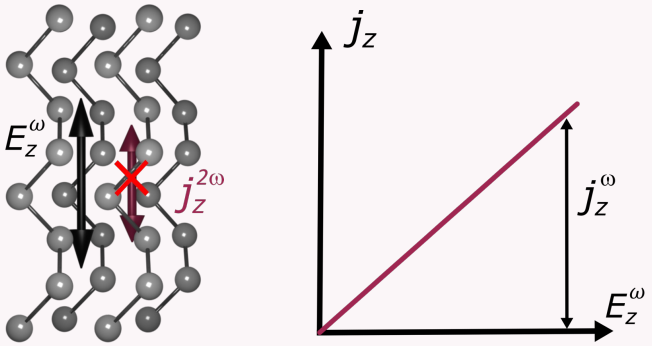
$$V^{2\omega} = R^{(2,0)}(I^{\omega})^2$$

$$\downarrow$$

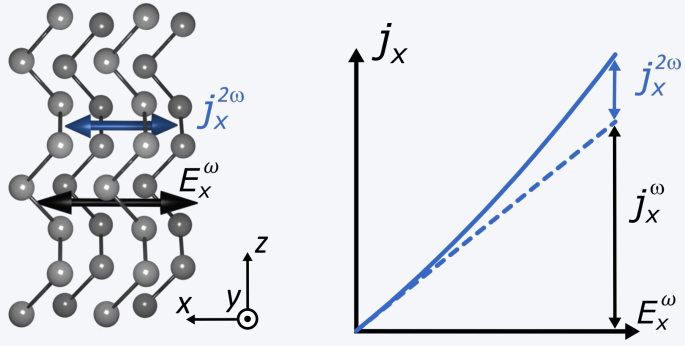
$$j_i^{2\omega} = \sigma_{ijk}^{(2,0)} E_j^{\omega} E_k^{\omega}$$

$$\sigma_{ijkl}^{(2,0)} = \begin{pmatrix} \sigma_{xxx}^{(2,0)} & \sigma_{xyy}^{(2,0)} & 0 & \sigma_{xyz}^{(2,0)} & 0 & 0 \\ 0 & 0 & 0 & 0 & \sigma_{yxz}^{(2,0)} & \sigma_{yxy}^{(2,0)} \\ 0 & 0 & 0 & 0 & 0 & 0 \end{pmatrix}$$

$$j_z = \sigma_{zz}^{(1,0)} E_z^{\omega}$$

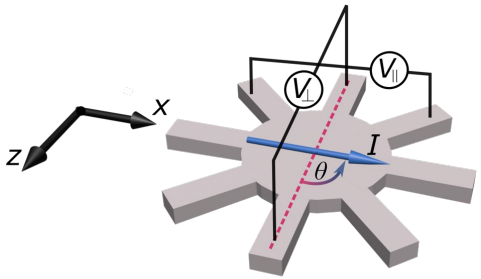


$$j_x = \sigma_{xx}^{(1,0)} E_x^{\omega} + \sigma_{xxx}^{(2,0)} E_x^{\omega} E_x^{\omega}$$



M. Suarez.-Rodriguez, LEH *et al.*, *Phys. Rev. Lett.* **132,** 046303 (2024)

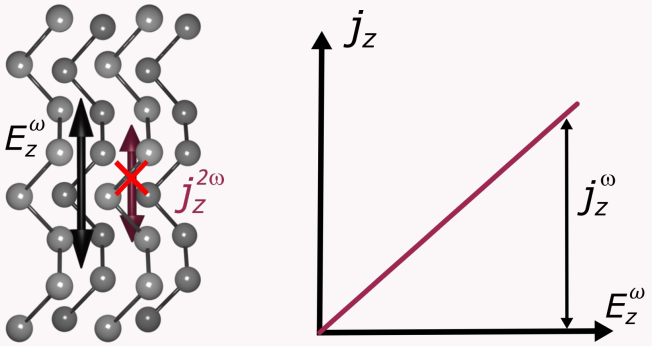
NLC in Te Symmetry origin



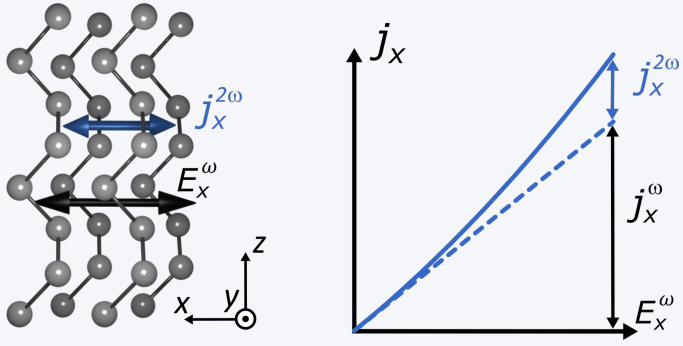
$$V_{\parallel}^{2\omega} = -\frac{L_{\parallel}}{2\sqrt{2}A^2}(\rho_{xx}^{(1,0)})^3\sigma_{xxx}^{(2,0)}(I^{\omega})^2 sin^3(\theta)$$

$$V_{\perp}^{2\omega} = -\frac{L_{\perp}}{2\sqrt{2}A^2}(\rho_{xx}^{(1,0)})^3\sigma_{xxx}^{(2,0)}(I^{\omega})^2 sin^2(\theta)\cos(\theta)$$

$$j_z = \sigma_{zz}^{(1,0)} E_z^{\omega}$$

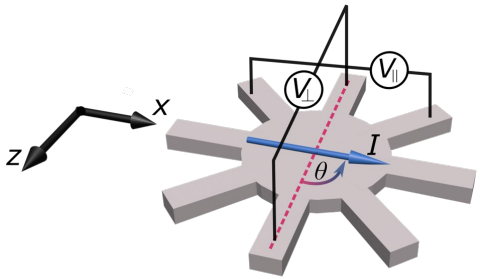


$$j_x = \sigma_{xx}^{(1,0)} E_x^{\omega} + \sigma_{xxx}^{(2,0)} E_x^{\omega} E_x^{\omega}$$



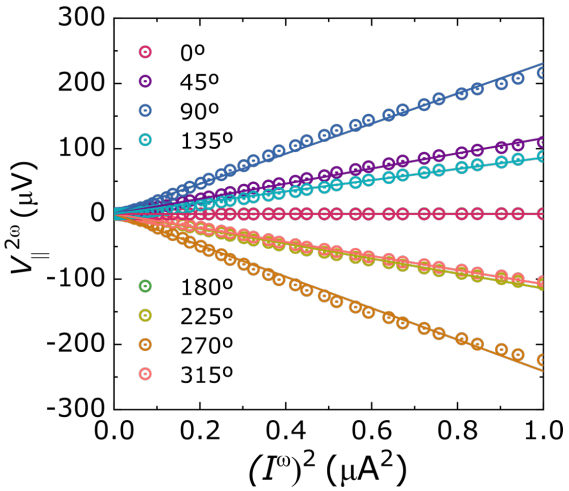
M. Suarez.-Rodriguez, LEH *et al., Phys. Rev. Lett.* **132,** 046303 (2024)

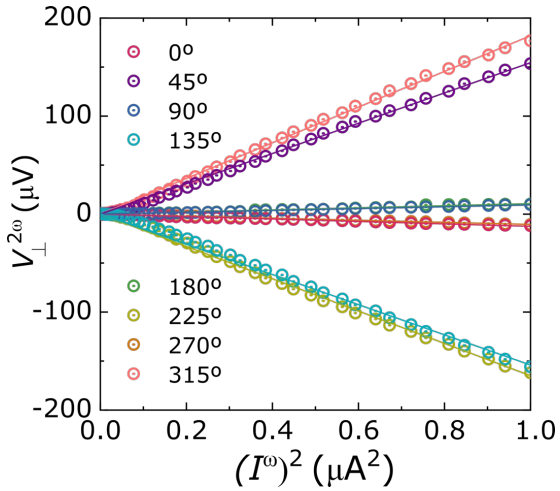
NLC in Te Experimental detection

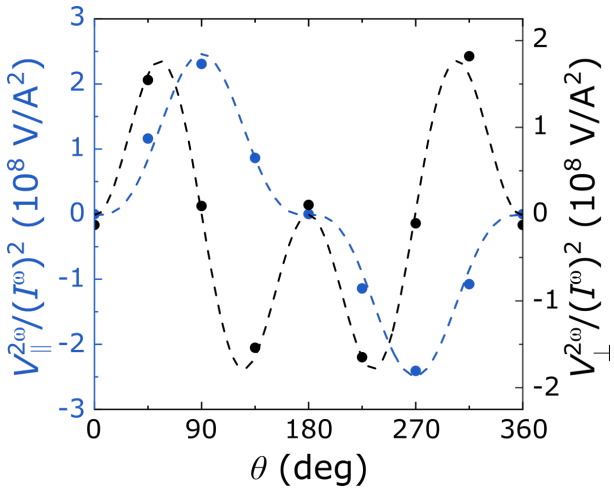


$$V_{\parallel}^{2\omega} = -\frac{L_{\parallel}}{2\sqrt{2}A^2}(\rho_{xx}^{(1,0)})^3\sigma_{xxx}^{(2,0)}(I^{\omega})^2 sin^3(\theta)$$

$$V_{\perp}^{2\omega} = -\frac{L_{\perp}}{2\sqrt{2}A^2}(\rho_{xx}^{(1,0)})^3\sigma_{xxx}^{(2,0)}(I^{\omega})^2 sin^2(\theta)\cos(\theta)$$

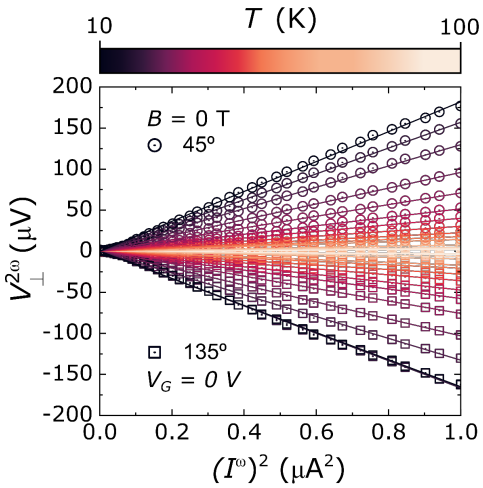


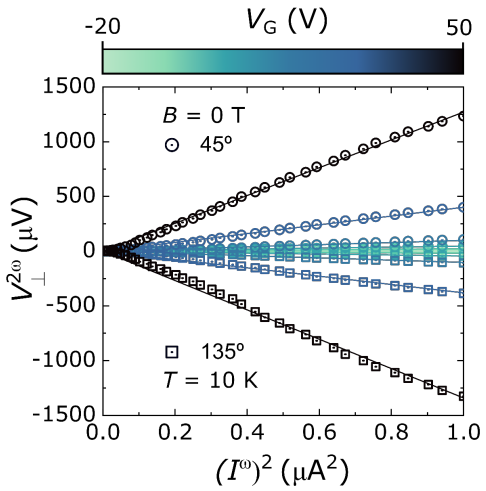


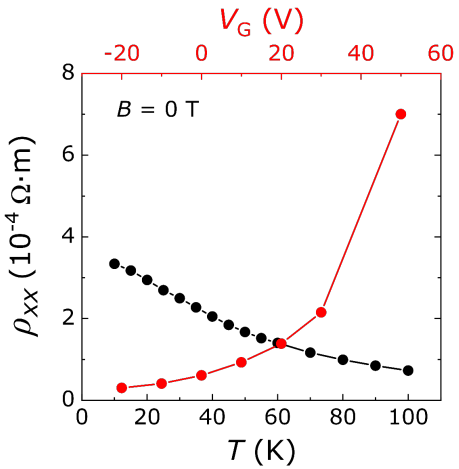


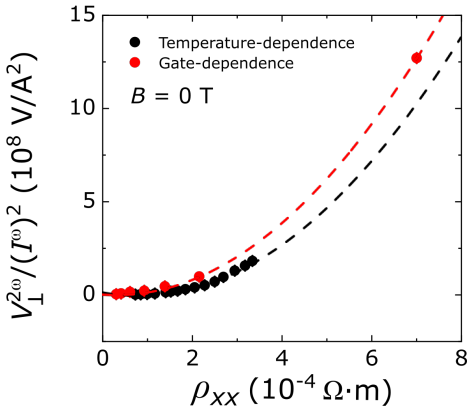
M. Suarez.-Rodriguez, LEH *et al., Phys. Rev. Lett.* **132,** 046303 (2024)

I NLC in Te Temperature and gate dependance. Scaling law









Scaling law:

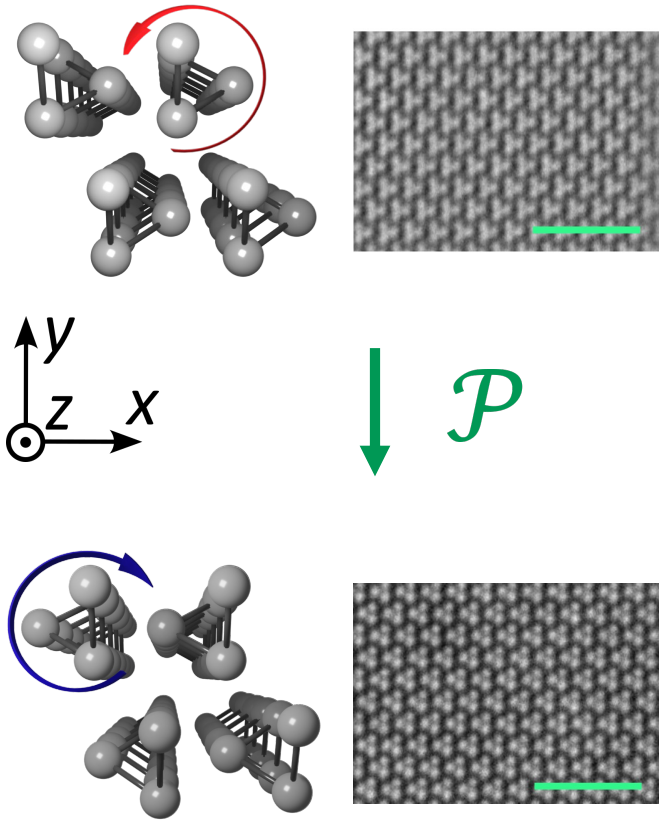
$$\frac{V_{\perp}^{2\omega}}{(I^{\omega})^2} = \beta + \gamma\rho_{xx} + \delta\rho_{xx}^2$$

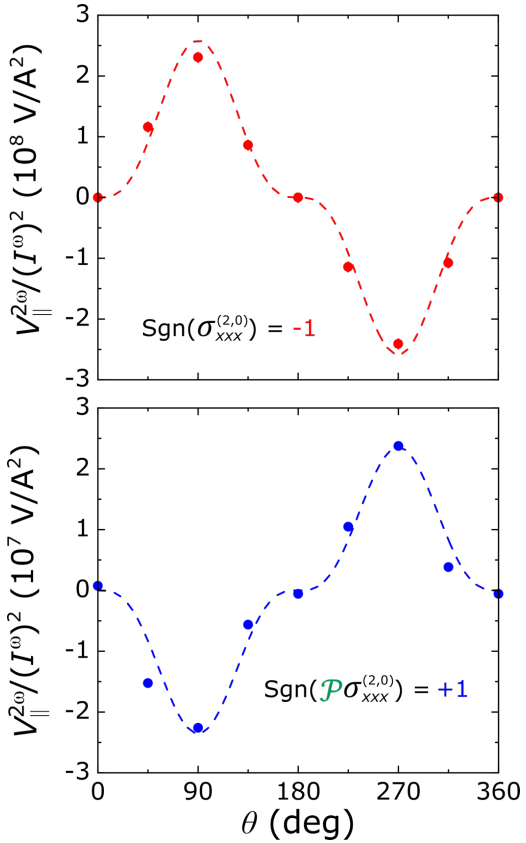
Du *et al.*, *Nat. Commun.* **3**, 3047 (2019)

Side-jump scattering from dynamic sources

M. Suarez.-Rodriguez, LEH *et al.*, *Phys. Rev. Lett.* **132,** 046303 (2024)

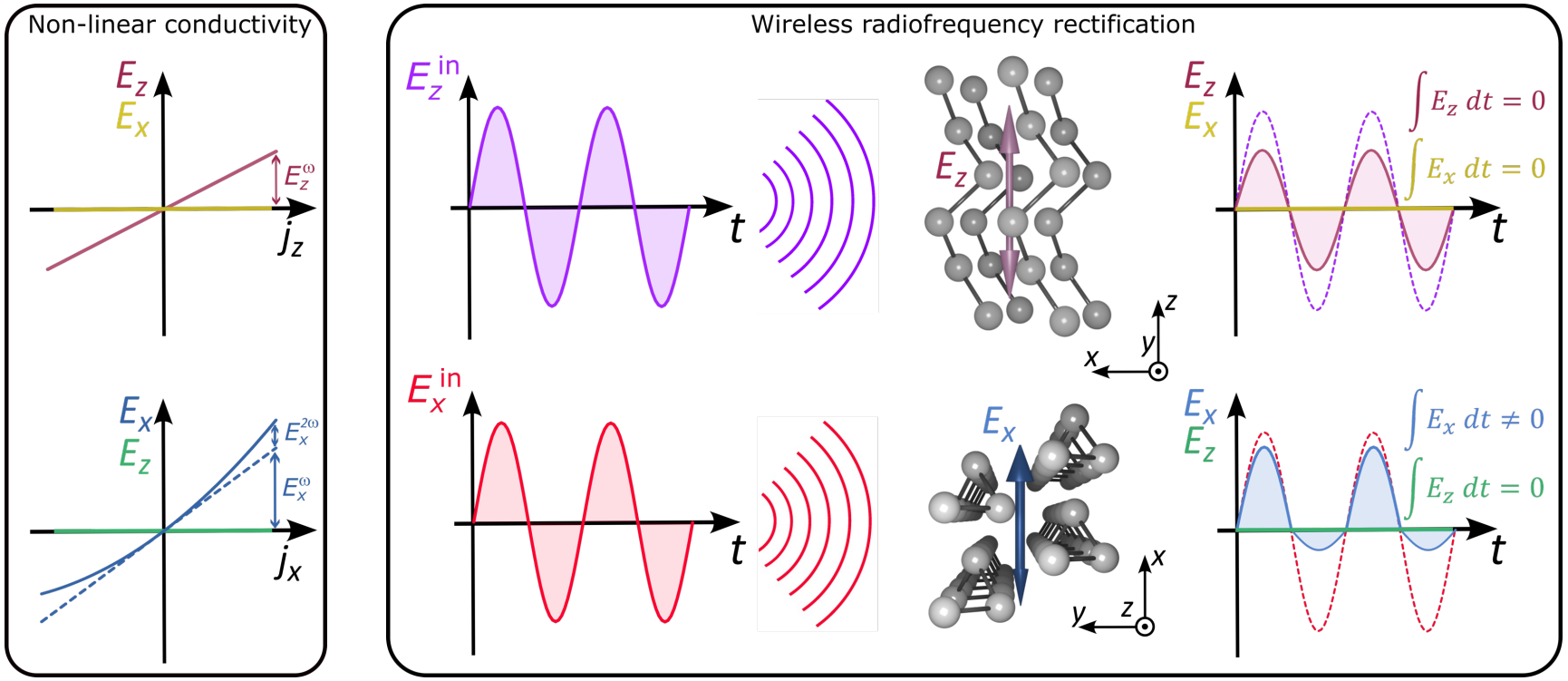
NLC in Te Inversion operation





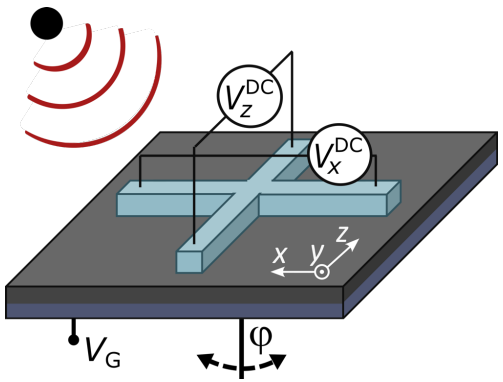
M. Suarez.-Rodriguez, LEH *et al., Phys. Rev. Lett.* **132,** 046303 (2024)

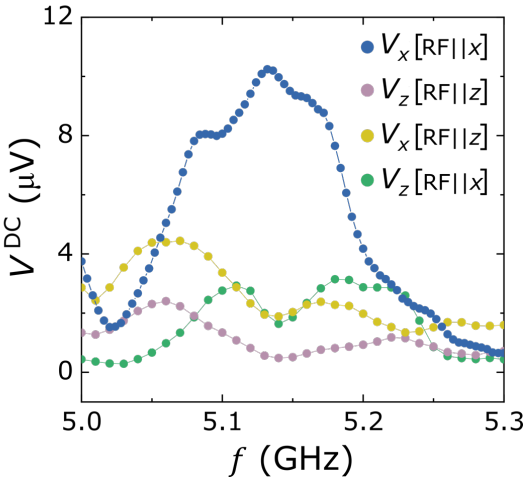
NLC in Te Applications – Energy harvesting

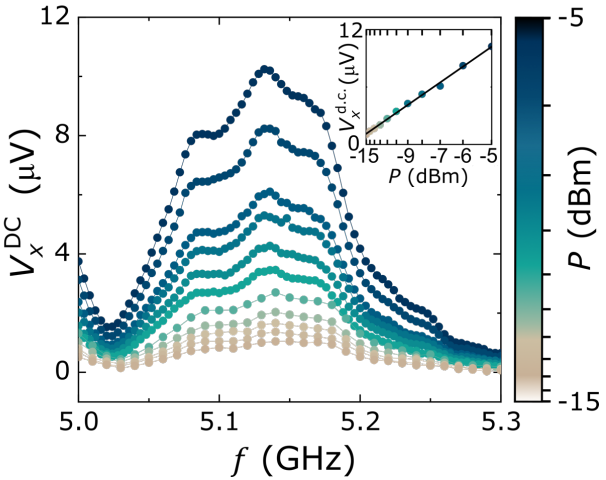


M. Suarez-Rodriguez, LEH *et al.*, *Adv. Mater.* **36,** 2400729 (2024)

NLC in Te Applications – Energy harvesting

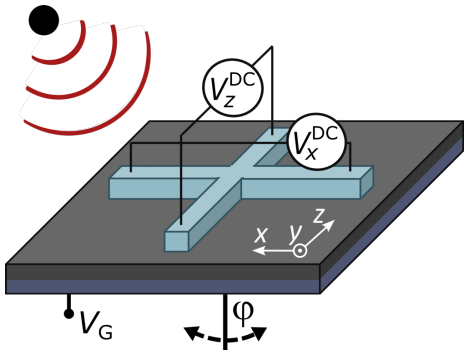






M. Suarez-Rodriguez, LEH *et al.*, *Adv. Mater.* **36,** 2400729 (2024)

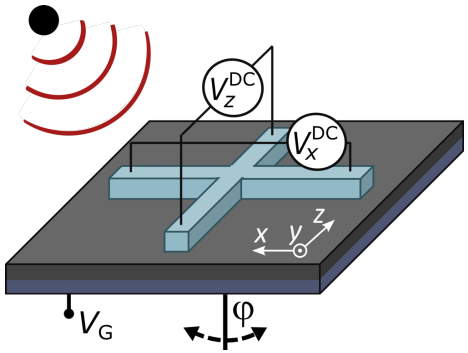
NLC in Te Applications – Energy harvesting

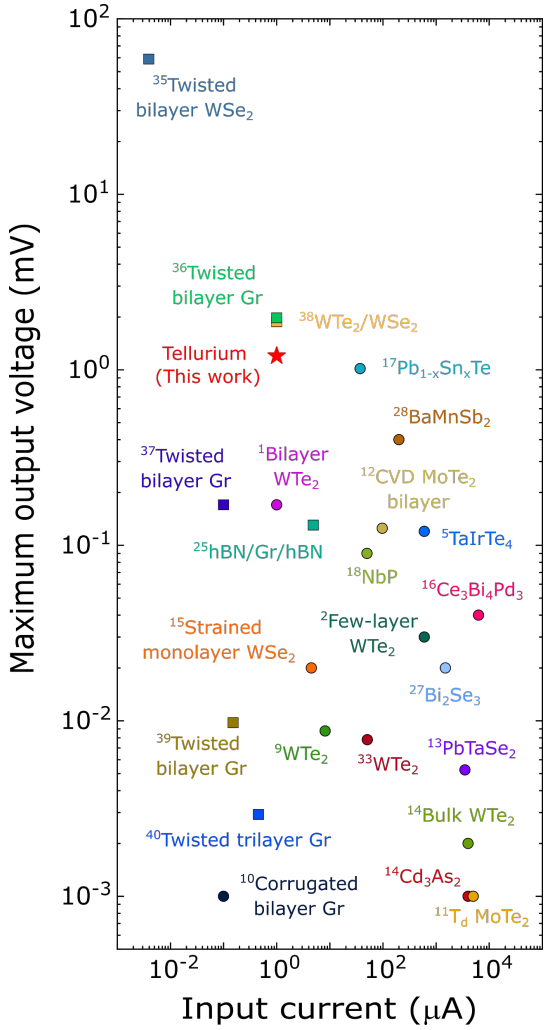


Material	Mechanism	T (K)	f (GHz)	P^{in} (nW)	P^{out} (nW)	η (%)
$TaIrTe_4$	BCD, extrinsic	300	2.45	0.9	0.02	0.023
$MnBi_2Te_4$	BCP	20	0.2-20	-	0.01	-
BiTeBr	Extrinsic	300	0.2-5.9	-	0.53	-
WTe_2	BCD	300	2.45	3	0.0015	0.0005
Bi_2Se_3	Extrinsic	300	2.45	15.2	0.18	0.01
Bi_2Te_3	Extrinsic	300	2.45-27.4	3.18	0.47	0.15
Te	Extrinsic	10-300	5.15	0.95	0.04	0.04

M. Suarez-Rodriguez, LEH *et al., Adv. Mater.* **36,** 2400729 (2024)

NLC in Te Applications – Energy harvesting





M. Suarez-Rodriguez, LEH *et al.*, *Adv. Mater.* **36,** 2400729 (2024)

Outline

Electronic transport

The case study: Chiral Te

Non-linear conductivity in Te

Non-linear magnetoconductivity in Te

Conclusions

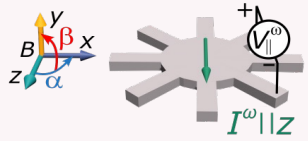
NLMC in Te Symmetry origin

$$V^{2\omega} = R^{(2,1)}(I^{\omega})^2 B$$

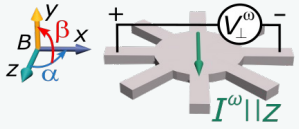
$$\downarrow$$

$$j_i^{2\omega} = \sigma_{ijkl}^{(2,1)} E_j^{\omega} E_k^{\omega} B_l$$

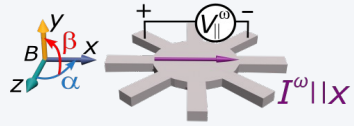
$$\sigma_{ijkl}^{(2,1)} = \begin{pmatrix} \sigma_{xxxx}^{(2,1)} & \sigma_{xzzx}^{(2,1)} & 0 \\ 0 & 0 & \sigma_{xxzy}^{(2,1)} \\ 0 & 0 & \sigma_{xxzz}^{(2,1)} \\ 0 & 0 & \sigma_{zxzx}^{(2,1)} \\ \sigma_{zxxy}^{(2,1)} & 0 & 0 \\ \sigma_{zxxz}^{(2,1)} & \sigma_{zzzz}^{(2,1)} & 0 \end{pmatrix}$$



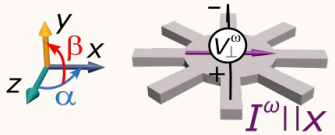
$$V_{\parallel}^{2\omega} = -\frac{L_{\parallel}}{2\sqrt{2}A^2}(\rho_{zz}^{(1,0)})^3 \sigma_{zzzz}^{(2,1)} (I^{\omega})^2 B cos(\alpha)\cos(\beta)$$



$$V_{\perp}^{2\omega} = -\frac{L_{\perp}}{2\sqrt{2}A^2}\rho_{xx}^{(1,0)}(\rho_{zz}^{(1,0)})^2 \sigma_{xzzx}^{(2,1)} (I^{\omega})^2 B sin(\alpha)\cos(\beta)$$



$$V_{\parallel}^{2\omega} = -\frac{L_{\parallel}}{2\sqrt{2}A^2}(\rho_{xx}^{(1,0)})^3 \sigma_{xxxx}^{(2,1)} (I^{\omega})^2 B sin(\alpha)\cos(\beta)$$



$$V_{\perp}^{2\omega} = -\frac{L_{\perp}}{2\sqrt{2}A^2}(\rho_{xx}^{(1,0)})^2 \rho_{zz}^{(1,0)} (I^{\omega})^2 B[\sigma_{zxxz}^{(2,1)} cos(\alpha)\cos(\beta) + \sigma_{zxxy}^{(2,1)} \sin(\beta)]$$

M. Suarez-Rodriguez, LEH *et al.*, *Phys. Rev. B* **111**, 024405 (2024)

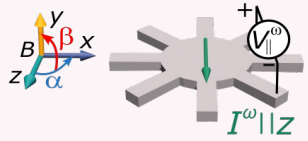
NLMC in Te Symmetry origin

$$V^{2\omega} = R^{(2,1)}(I^{\omega})^2 B$$

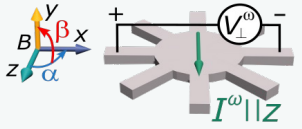
$$\downarrow$$

$$j_i^{2\omega} = \sigma_{ijkl}^{(2,1)} E_j^{\omega} E_k^{\omega} B_l$$

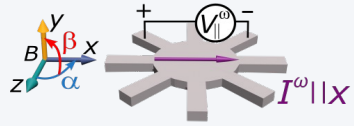
$$\sigma_{ijkl}^{(2,1)} = \begin{pmatrix} \sigma_{xxxx}^{(2,1)} & \sigma_{xzzx}^{(2,1)} & 0 \\ 0 & 0 & \sigma_{xxzy}^{(2,1)} \\ 0 & 0 & \sigma_{xxzz}^{(2,1)} \\ 0 & 0 & \sigma_{zxzx}^{(2,1)} \\ \sigma_{zxxy}^{(2,1)} & 0 & 0 \\ \sigma_{zxxz}^{(2,1)} & \sigma_{zzzz}^{(2,1)} & 0 \end{pmatrix}$$



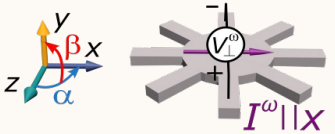
$$V_{\parallel}^{2\omega} = -\frac{L_{\parallel}}{2\sqrt{2}A^2}(\rho_{zz}^{(1,0)})^3 \sigma_{zzzz}^{(2,1)} (I^{\omega})^2 B cos(\alpha)\cos(\beta)$$



$$V_{\perp}^{2\omega} = -\frac{L_{\perp}}{2\sqrt{2}A^2}\rho_{xx}^{(1,0)}(\rho_{zz}^{(1,0)})^2 \sigma_{xzzx}^{(2,1)} (I^{\omega})^2 B sin(\alpha)\cos(\beta)$$



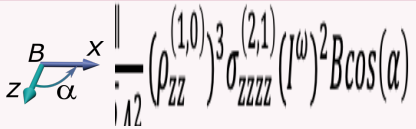
$$V_{\parallel}^{2\omega} = -\frac{L_{\parallel}}{2\sqrt{2}A^2}(\rho_{xx}^{(1,0)})^3 \sigma_{xxxx}^{(2,1)} (I^{\omega})^2 B sin(\alpha)\cos(\beta)$$



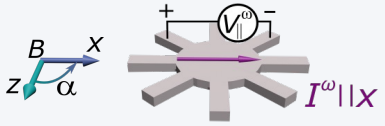
$$V_{\perp}^{2\omega} = -\frac{L_{\perp}}{2\sqrt{2}A^2}(\rho_{xx}^{(1,0)})^2 \rho_{zz}^{(1,0)} (I^{\omega})^2 B[\sigma_{zxxz}^{(2,1)} cos(\alpha)\cos(\beta) + \sigma_{zxxy}^{(2,1)} \sin(\beta)]$$

M. Suarez-Rodriguez, LEH *et al.*, *Phys. Rev. B* **111**, 024405 (2024)

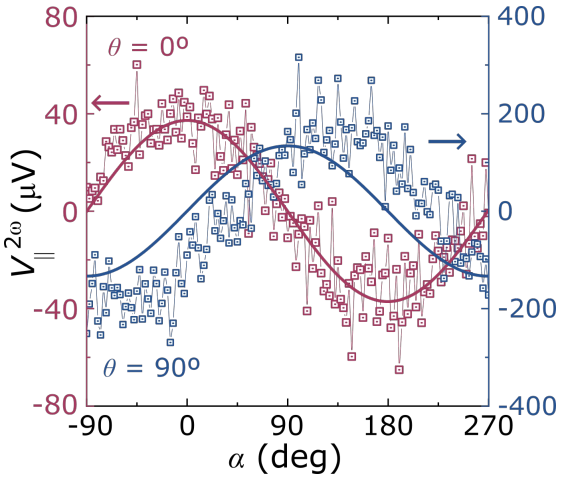
NLMC in Te Symmetry origin



$$V_{\parallel}^{2\omega} = -\frac{L_{\parallel}}{2\sqrt{2}A^2}(\rho_{zz}^{(1,0)})^3\sigma_{zzzz}^{(2,1)}(I^{\omega})^2 B\cos(\alpha)$$

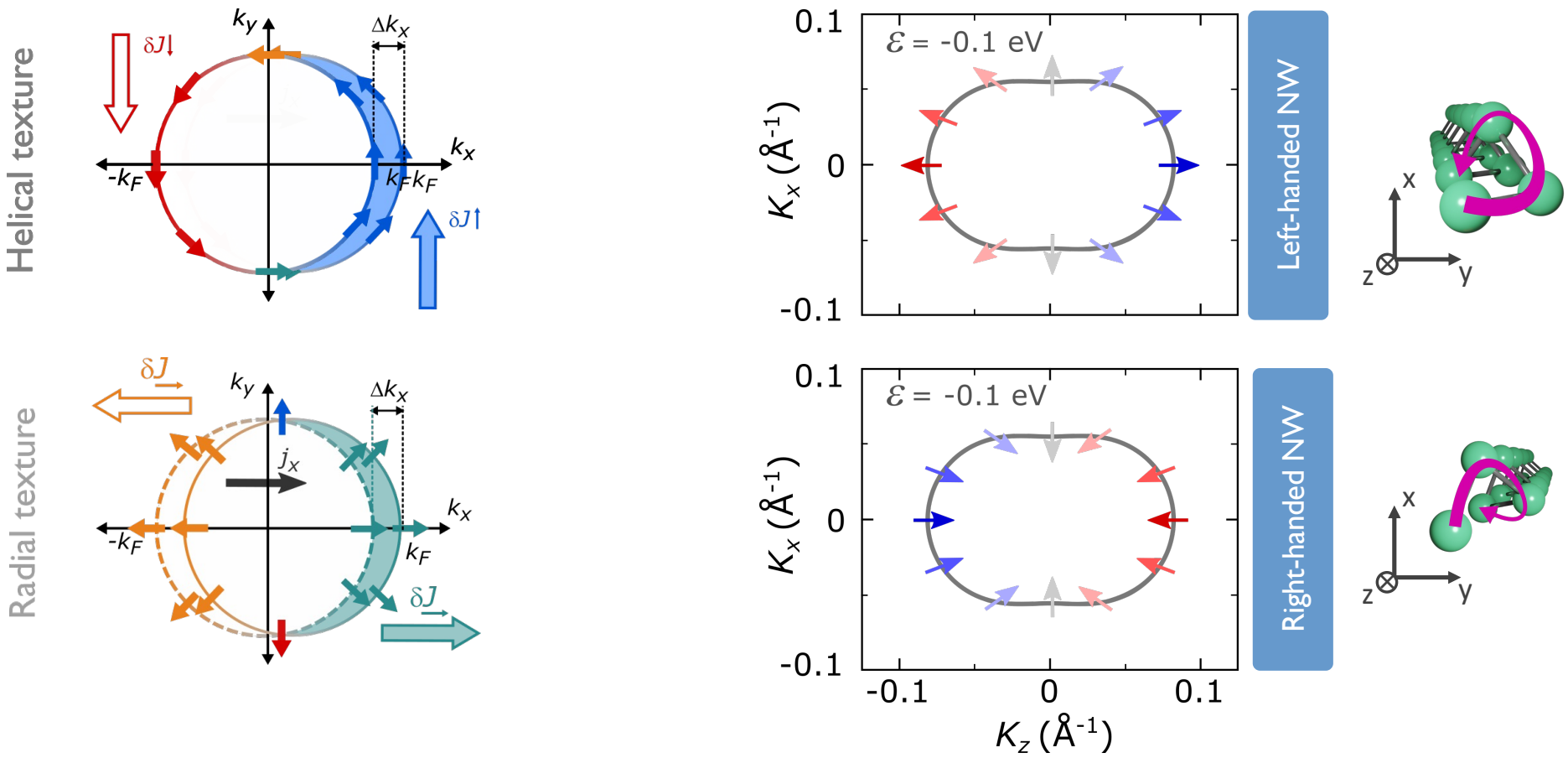


$$V_{\parallel}^{2\omega} = -\frac{L_{\parallel}}{2\sqrt{2}A^2}(\rho_{xx}^{(1,0)})^3\sigma_{xxxx}^{(2,1)}(I^{\omega})^2 B\sin(\alpha)$$

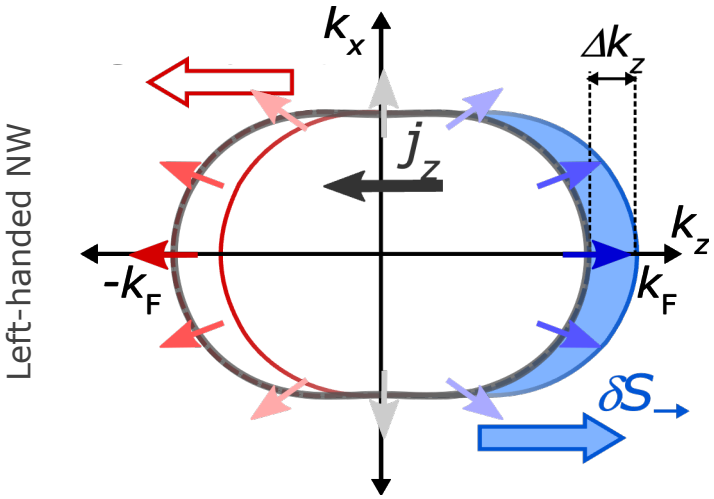


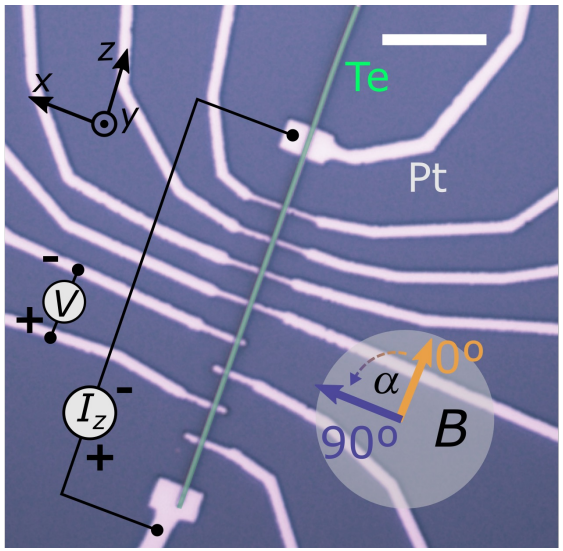
M. Suarez-Rodriguez, LEH *et al.*, *Phys. Rev. B* **111**, 024405 (2024)

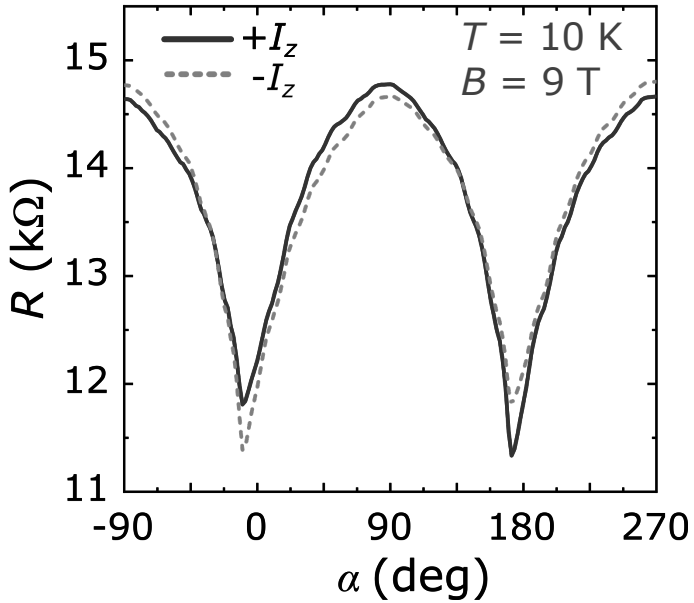
NLMC in Te Applications - Spintronics



NLMC in Te Applications - Spintronics





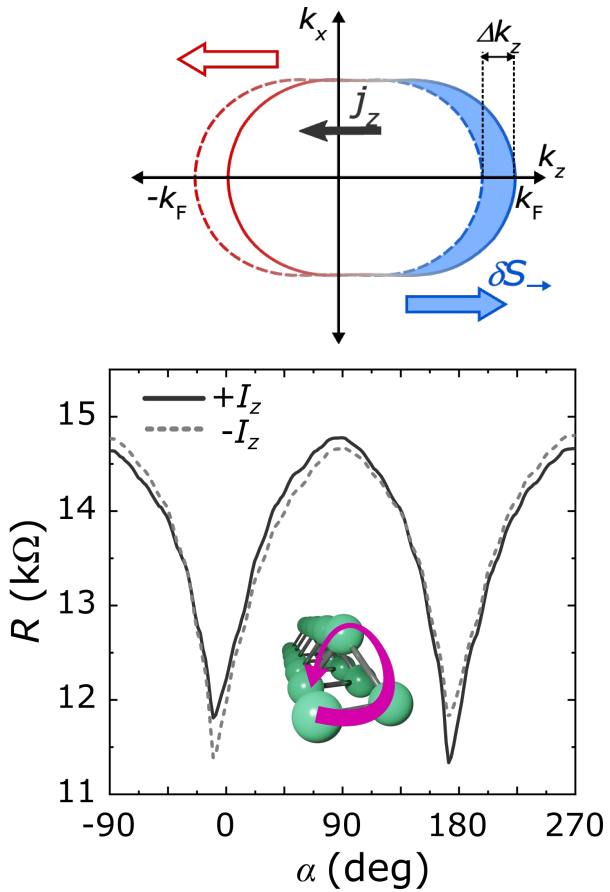


Resistance depends on the relative alignment between I_z and B

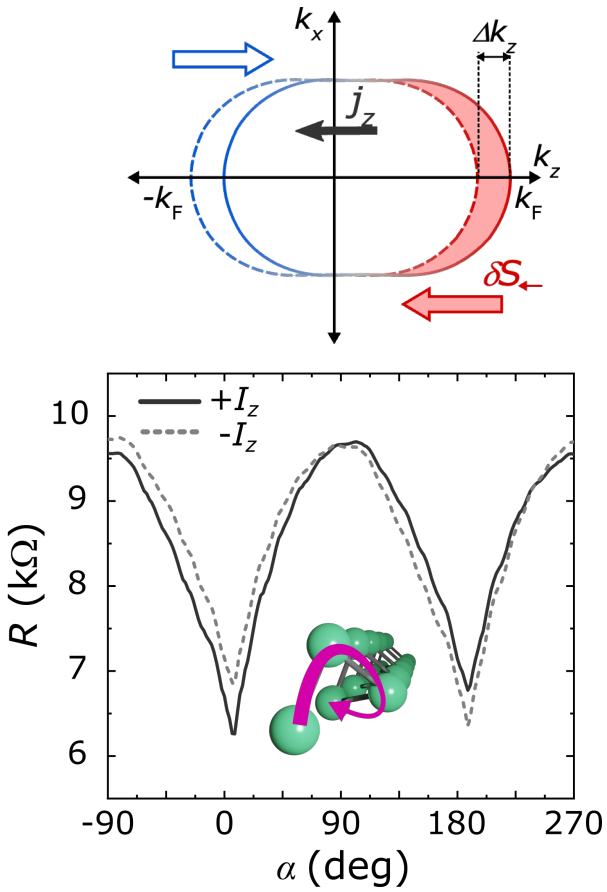
Unidirectional Magnetoresistance / Non-reciprocal charge transport / Chiral Induced Spin selectivity

NLMC in Te Applications - Spintronics

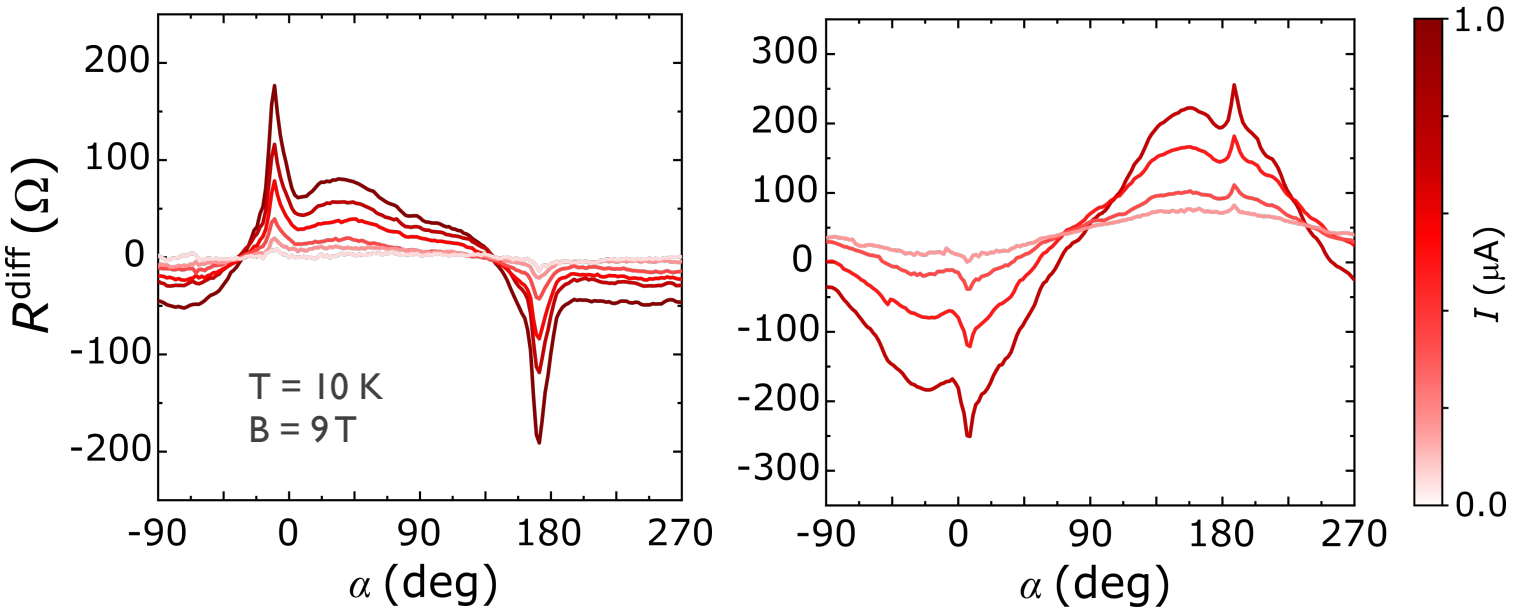
Left-handed NW



Right-handed NW



NLMC in Te Applications - Spintronics



Left-handed

Right-handed

Spin-polarization depends on the chirality

NLMC in Te Applications - Spintronics

$$\eta = \frac{R^{2\omega}}{R_0 j B}$$

Material	Spin Texture	Type	η (cm^2 A^{-1} T^{-1})	
Tellurium	**Radial**	**Chiral material**	**4 x 10^{-6}**	**Our work**
Ge (111)	Helical	Rashba surface	4.2 x 10^{-7}	Phys. Rev. Lett. **124**, 027201 (2020)
BiTeBr	Helical	Polar semiconductor	3 x 10^{-8}	Nat. Phys. **13**, 578 (2017)
SrTiO3	Helical	Rashba surface	4.2 x 10^{-8}	Phys. Rev. Lett. **120**, 266802 (2018)
α- GeTe	Helical	Rashba surface and bulk	7.1 x 10^{-10}	Nat. Commun. **12**, 540 (2021)
Bi_2Se_3	Helical	Topological insulator	5.9 x 10^{-11}	Nat. Phys. **14**, 495 (2018)
WTe_2	Helical	Topological semimetal	1 x 10^{-13}	Nat. Commun. **10**, 1290 (2019)
CoPt	Helical	Rashba bulk	5.9 x 10^{-14}	Phys. Rev. B **107**, 094410 (2023)

F. Calavalle†, M. Suarez-Rodriguez† , LE.H *et al., Nat. Mater.* **21**, 526 (2022)

Conclusions

- Vast phenomenology of non-linear transport in non-centrosymmetric materials
- Tellurium as a playground chiral material
- Non-linear conductivity leads to energy harvesting applications
- Non-linear magnetoconductivity leads to the generation of spin polarization
- Extension to many other posible (artificial) chiral systems

Conclusions

Non-linear conductivity in graphene twisted structures
Advanced Materials, e09837 (2025)
ACS Nano 19, 24930 (2025)
Small 21, 2501426 (2025)

Bulk Photovoltaic effect in 2D materials without inversion symmetry
NanoLetters 24, 14728 (2024)

Spin polarization and anomalous non-linear magnetoconductivity in 2D structures
Advanced Materials 37, 2419283 (2025)
Nature Materials 23, 1502 (2024)
Advanced Materials 36, 2310768 (2024)

Extension to many other posible (artificial) chiral systems